ICES Journal of Marine Science, 2023, **0**, 1–12
DOI: 10.1093/icesjms/fsad013
Original Article

Vertebrae reveal industrial-era increases in Atlantic bluefin tuna catch-at-size and juvenile growth

Adam J. Andrews [1,*], Antonio Di Natale [2], Piero Addis [3], Federica Piattoni [1], Vedat Onar [4], Darío Bernal-Casasola [5], Veronica Aniceti [6], Gabriele Carenti [7], Verónica Gómez-Fernández [8], Fulvio Garibaldi [9], Arturo Morales-Muñiz [10,*] and Fausto Tinti [1]

[1]Department of Biological, Geological and Environmental Sciences,University of Bologna, 48123 Ravenna,Italy
[2]Aquastudio Research Institute, 98121 Messina ME, Italy
[3]Department of Life and Environmental Sciences, University of Cagliari,09124 Cagliari, Sardinia,Italy
[4]Osteoarchaeology Practice and Research Centre, Faculty of Veterinary Medicine, Istanbul University-Cerrahpaşa,34320 Istanbul,Turkey
[5]Department of History, Geography and Philosophy, Faculty of Philosophy and Letters, University of Cádiz, 11003. Cádiz,Spain
[6]Museum of Natural History, University of Bergen, 5007 Bergen, Norway
[7]CEPAM, CNRS, Université Côte d'Azur, 06357 Nice,France
[8]I.N.I.C.E—Instituto Nacional de investigaciones científicas y ecológicas, 37008 Salamanca,Spain
[9]Department of Earth, Environment and Life Sciences (DISTAV), University of Genoa,16182 Genoa,Italy
[10]Department of Biology, Autonomous,University of Madrid,28049 Madrid,Spain

[*] *Corresponding authors: tel: +39 0544 937311;* e-mails: adam@palaeome.org, arturo.morales@uam.es.

Climate change and size-selective overexploitation can alter fish size and growth, yet our understanding of how and to what extent is limited due to a lack of long-term biological data from wild populations. This precludes our ability to effectively forecast population dynamics and support sustainable fisheries management. Using modern, archived, and archaeological vertebrae dimensions and growth rings of one of the most intensely exploited populations, the eastern Atlantic and Mediterranean bluefin tuna (*Thunnus thynnus*, BFT), we estimated catch-at-size and early-life growth patterns from the 3 rd century bce to the 21 st century ce to understand responses to changes in its environment. We provide novel evidence that BFT juvenile growth increased between the 16 th –18 th , 20 th , and 21 st centuries, and is correlated with a warming climate and likely a decrease in stock biomass. We found it equally plausible that fisheries-induced evolution has acted to increase juvenile BFT growth, driving earlier maturation as a result of size-selective exploitation. Coincidently, we found limited evidence to suggest a long history of large (>200 cm FL) BFT capture. Instead, we found that the catch-at-size of archaeological BFT was relatively small in comparison with more intensive, 20 th and 21 st century tuna trap fisheries which operated further from shore. This complex issue would benefit from studies using fine-scale biochronological analyses of otoliths and adaptation genomics, throughout the last century especially, to determine evolutionary responses to exploitation, and further disentangle the influence of temperature and biomass on fish growth.

Keywords: climate change, fisheries-induced evolution, fish trait plasticity, growth of fishes, historical baselines, historical fish size, *Thunnus thynnus*.

Introduction

In light of ocean warming and the recent overexploitation of fish stocks, long-term investigations into how climate and exploitation affected fish trait plasticity and adaptation in the past are crucial to predict population dynamics and thereby support sustainable fisheries management (Law, 2000; Jørgensen *et al.*, 2007; Lotze *et al.*, 2014; Rodrigues *et al.*, 2019). In particular, the key traits of fish size and growth affect many metrics used to assess stocks, such as size at maturation, fecundity, recruitment, and biomass (Fromentin, 2003; Jørgensen *et al.*, 2007), and display various responses in relation with climatic and exploitation conditions on decadal and centennial scales (Bolle *et al.*, 2004; Enberg *et al.*, 2012; van der Sleen *et al.*, 2016; Ólafsdóttir *et al.*, 2017; Barrett, 2019; Denechaud *et al.*, 2020; Vieira *et al.*, 2020). One of the most intensely and longest exploited fishes is the Atlantic bluefin tuna (*Thunnus thynnus*; BFT); commercial exploitation began ca. 8th c. BCE for its eastern Atlantic and Mediterranean stock (Di Natale, 2014; Porch *et al.*, 2019; Andrews *et al.*, 2022b), and by 2007, this stock was considered depleted (ICCAT, 2007). Moreover, its spawning and feeding habitats rank among the fastest-warming ocean regions (Giorgi, 2006). Despite this, there is hitherto no information on the long-term temporal variation in BFT size or growth.

Here, we fill this data gap by reconstructing pre-industrial catch-at-size data using archaeological vertebrae, and by analysing the early-life growth of archaeological, archived, and modern specimens using vertebrae annuli (annual growth ring) measurements, spanning centuries, to determine how and why growth varies over time for the eastern Atlantic and Mediterranean stocks of BFT. A lack of temporal samples for the western Atlantic stock, owing to the later onset of its commercial exploitation (Andrews *et al.*, 2022b), precludes its inclusion here.

Historical catch-at-size data, collated from records or reconstructed using archaeological bone measurements, inform on the gears used and sizes targeted in historical fisheries, in addition to stock age or size shifts over time (Maschner *et al.*, 2008; Plank *et al.*, 2018; Barrett, 2019; Sanchez, 2020). Size-selective overexploitation appears to have truncated the

Received: October 3, 2022. **Revised:** January 18, 2023. **Accepted:** January 19, 2023

size-structure of eastern BFT during the last 70 years (Fromentin, 2009; MacKenzie *et al.*, 2009; Siskey *et al.*, 2016b), and since this has the potential to alter fish growth (Law, 2000; Jørgensen *et al.*, 2007; Hollins *et al.*, 2018), pre-industrial catch-at-size baselines are vital to investigate demographics when the stock was less exploited and assess potential evolutionary impacts on growth.

Several decadal- and centennial-scale studies have shown that temporal changes in fish growth may result from plastic responses to ecological or environmental factors like biomass (Vieira *et al.*, 2020; Pedersen *et al.*, 2022), predator-prey interactions (Smoliński, 2019), or temperature (Geffen *et al.*, 2011; van der Sleen *et al.*, 2016; Denechaud *et al.*, 2020; Smoliński *et al.*, 2020), as well as evolutionary ones like fisheries-induced evolution (FIE) (Edeline *et al.*, 2007; Mollet *et al.*, 2007; Swain *et al.*, 2007; Neuheimer and Taggart, 2010; Saura *et al.*, 2010). FIE is the artificial selection of traits (early maturation and/or slow mature growth) that enhance survival and the number of offspring of individuals subject to fishing that commences above a certain size-threshold (Law, 2000; Enberg *et al.*, 2012). Empirical evidence of FIE is still lacking at the genomic level [with two exceptions: Therkildsen *et al.* (2019) and Czorlich *et al.* (2022)]; however, challenges in detecting polygenic adaptation and the infancy of historical genomic methods (Pinsky *et al.*, 2021) mean that FIE cannot be ruled out for intensely exploited marine fishes (Hutchings and Kuparinen, 2021). Yet, long-term phenotypic perspectives on how long size-selective harvesting has occurred and what impact this may have on growth remain scarce due to difficulties in obtaining temporal samples.

Typically, temporal patterns in fish growth are studied by assessing size-at-age [e.g. Campana (1990)] or the increment width of annuli [e.g. Morrongiello and Thresher (2015)] using otoliths; collected between years, decades, or centuries. Because archaeological BFT otoliths are yet to be recovered (Andrews *et al.*, 2022b), and we had access to archived BFT vertebrae (but no otoliths), collected ∼ 100 years ago by the ecologist Massimo Sella for his seminal size-at-age work (Sella, 1929), vertebrae were chosen as an alternative. Given that the reliability of size-at-age would be hindered by a ±10% error in reconstructing size using vertebrae (Andrews *et al.*, 2022a), and that BFT vertebra annuli are difficult to distinguish at vertebra centra edges, we opted for an increment size approach inspired by (Lee *et al.*, 1983). This required some consideration given that vertebrae (unlike otoliths) are subject to resorption (Campana and Thorrold, 2001). However, there is some precedent in using bone elements subject to resorption in long-term growth studies, such as vertebrae (Van Neer *et al.*, 1999) and scales (Guillaud *et al.*, 2017), indeed BFT fin-spine annuli have also been used to good effect to study growth (Landa *et al.*, 2015).

Since annuli have been validated as annual formations in BFT otoliths (Rodríguez-Marín *et al.*, 2007; Neilson and Campana, 2008; Siskey *et al.*, 2016a), and since vertebrae and otolith annuli closely correspond (until age 10) in southern bluefin tuna (*Thunnus maccoyii*, Gunn *et al.*, 2008), vertebra growth rings are likely annual in BFT at least until age 10. Given that BFT vertebra centra are highly correlated with fork length (FL) (Rodríguez-Roda, 1964; Lee *et al.*, 1983; Andrews *et al.*, 2022a), vertebra annuli increment sizes can also be considered to be proportional to somatic growth. A lack of sex information for historical specimens should also not be a hinderance to our study since sexual dimorphism only occurs between large BFT (Santamaria *et al.*, 2009; Addis *et al.*, 2014; Stewart *et al.*, 2022). Therefore, we find no reason to omit the opportunity to study long-term growth in BFT, provided that we assess the relationship between increment size and vertebrae size to ensure interpretations can be made of increment sizes from different sized vertebrae in BFT.

Despite considerable interest in this large [up to 3.3 m in length and 725 kg in weight: Cort *et al.* (2013)], highly migratory species, as detailed in several solid reviews (Mather *et al.*, 1995; Cort, 2003; Fromentin, 2003, 2009; Cort *et al.*, 2013; Murua *et al.*, 2017), long-term growth data is lacking. Long-term insights on growth patterns in BFT would be of practical significance due to their consequences for fisheries management. Size-at-age has been well-studied in BFT since Sella's time (Sella, 1929), most notably by (Rodríguez-Roda, 1964; Cort, 1989; Rodríguez-Marín *et al.*, 2006), and published growth-curves for the eastern BFT stock [summarized in Cort *et al.* (2014) reveal variation between studies but no temporal trend (Supplementary Figure 1, Restrepo *et al.* (2007)]. Due to the biological trade-off between fish growth and maturation (Enberg *et al.*, 2012), studying one of these traits can be indicative of the other; however, no study has addressed temporal age-at-maturation changes in eastern BFT, either, where the original theory persists, that is, maturation beginning at age 3, while all individuals are mature by age 5 (Rodríguez-Roda, 1967; Mather *et al.*, 1995; Corriero *et al.*, 2005). Fromentin (2003) is the only study on BFT to note temporal variation in size-at-age, noting that juvenile weight-at-age decreased between 1982 and 1998, which we hope to shed light on here.

In the present study, we investigate pre-industrial BFT catch-at-size to inform on the size-selectivity and impact of their exploitation history and test the hypothesis that BFT growth varies temporally in response to environmental conditions or size-selective exploitation (FIE). To this end, our objectives were to (1) reconstruct the size of archaeological BFT using vertebra measurements and discuss these in relation with those collated in recent decades by ICCAT, and (2) assess changes in early-life BFT growth using archaeological, archived, and modern vertebrae annuli and attempt to characterize these in terms of plastic or evolutionary responses.

Materials and methods

Historical catch-at-size estimation

To obtain catch-at-size estimates for the historical era, 286 BFT vertebrae were sampled from nine archaeological sites in the eastern Atlantic and Mediterranean, each dated by archaeological context or radiocarbon, between the 3 rd century BCE–18 th century CE (Table 1, Figure 1: for details see Supplementary Materials). Care was taken to avoid sampling the same individual twice by selecting a single vertebra when several were in anatomical position, and vertebrae of different sizes and levels of preservation (assessed visually) when selecting from each stratigraphic unit. Small (<100 cm FL) specimens were not sampled because their morphological identification to species level is not considered reliable, as they may represent albacore (*Thunnus alalunga*) and were thus excluded.

FL of archaeological specimens was estimated following Andrews *et al.* (2022a) using the online resource https://tunaarchaeology.org/lengthestimations. Briefly, vertebrae were

Table 1. Summary of modern, archival, and archaeological Atlantic bluefin tuna (*T. thynnus*) vertebra sample details used in FL estimations and growth analyses in the current study. V35: 35th ranked vertebra, V36: 36th ranked vertebra.

Sample ID/Year	Archaeological sample site or fishing location	Long.	Lat.	*n* vertebrae sampled for growth	*n* V35 specimens analysed for growth	*n* V36 specimens analysed for growth	*n* vertebrae used in FL estimation	FL min-max (mean) cm
2020 CE	Carloforte, Sardinia, Italy	8.31	39.18	58	29	29	–	98–197 (124)
2020 CE	Ligurian Sea, Italy	8.21	43.62	56	28	27	–	104–165 (131)
1926 CE	Venice, Veneto, Italy	14.59	43.93	46	18	15	–	114–187 (143)
1925 CE	Zliten, Libya	14.66	33.25	42	20	15	–	115–249 (182)
1911–1912 CE	Pizzo/Messina, Italy	15.34	38.97	45	21	20	–	78–154 (107)
16th–18th c. CE	Pedras de Fogu, Sardinia, Italy	8.62	40.86	21	13	8	38	99–232 (153)
1755 CE	La Chanca, Conil, Spain	−6.09	36.28	23	13	10	30	140–228 (182)
13th c. CE	Mazara del Vallo, Sicily, Italy	12.58	37.65	–	–	–	6	140–230 (172)
9th–13th c. CE	Yenikapi, Istanbul, Turkey	28.95	41.01	–	–	–	60	131–284 (200)
10th–11th c. CE	Palermo∗, Sicily, Italy	13.37	38.11	–	–	–	20	101–185 (138)
4th–5th c. CE	Baelo Claudia, Spain	−5.77	36.09	–	–	–	21	107–210 (137)
1st–4th c. CE	Portopalo, Sicily, Italy	15.13	36.68	–	–	–	14	118–227 (159)
1st c. CE	Olivillo, Spain	−6.31	36.53	–	–	–	24	90–164 (132)
2nd c. BCE	Punta Camarinal, Spain	−5.77	36.09	6	3	3	59	138–213 (151)
3rd c. BCE	Portopalo, Sicily, Italy	15.13	36.68	7	4	3	14	103–261 (178)

∗ Palermo samples pertain to two different archaeological sites (see Supplementary Materials for details). *n* = number. Lat. = Latitude. Long. = Longitude.

identified to rank or type [see Andrews *et al.* (2022a)], vertebrae centra length, width, and height were measured using digital callipers to the nearest 0.01 mm, and the best-fitting power regression model was applied for each specimen (Figure 1, Supplementary Table S1), which predicts FL to ca. 90% accuracy. When centra were damaged by post-mortem processes, prohibiting the measurement of one or more dimensions, the next-best scoring dimension model was applied. A comparative FL dataset for the 20th–21st century CE tuna trap fishery (Supplementary Table S2) was obtained from ICCAT (www.iccat.int/en/accesingdb.html), including 1915–1927 FL data ($n = 253$) from Italian and Libyan tuna traps, initially published by (Pagá Garcia *et al.*, 2017).

Growth estimation: sample collection

To estimate temporal variation in BFT growth, we identified archaeological, archived, and modern BFT vertebrae to rank [see Andrews *et al.* (2022a)] and collected the 35th (V35) and 36th (V36) vertebrae as these often show clearly-defined annuli (growth rings) and thus have a long history of use in BFT ageing (Sella, 1929; Galtsoff, 1952; Rodríguez-Roda, 1964; Lee *et al.*, 1983; Rodríguez-Marín *et al.*, 2006). A total of 57 archaeological specimens with sufficient preservation were collected from four sites and two periods, namely the 3rd–2nd c. BCE (Portopalo and Punta Camarinal) and 16th–18th c. CE (La Chanca and Pedras de Fogu) (Table 1, Figure 1: for details see Supplementary Materials).

A total of 133 archival BFT vertebrae (Massimo Sella Archive, University of Bologna) were selected, pertaining to three central Mediterranean tuna trap sites/years during the early 20 th c. (Table 1, Figure 1). These sample groups were 1911–1912 (Pizzo and Messina, Italy), 1925 (Venice, Italy), and 1926 (Zilten, Libya). Archived vertebrae were stored dry after the removal of soft tissues by unknown means. A total of 121 modern specimens were obtained from longlines off Sanremo and Imperia (Italy, $n = 28$) as bycatch of a swordfish (*Xiphias gladius*) longline fishery, and tuna-trap off Isola Piana (Carloforte, Sardinia: Carloforte Tonnare PIAM srl., Italy, $n = 29$), in June–October 2020, and May 2020, respectively. Modern vertebrae were mechanically cleaned of soft tissues, macerated in ambient-temperature water for up to 2 months to remove soft tissues by microbial decomposition, then dried before analyses were conducted to mimic the treatment of archaeological and archival specimens.

Growth estimation: specimen preparation and measurement

To estimate the FL of individuals used in growth analyses and to study the relationship between vertebrae size and annuli increment widths, measurements of vertebra centra length, width, and height were made using digital callipers to the nearest 0.01 mm. The height and width of vertebrae were measured on the posterior centrum of V35 and the anterior centrum of V36. Vertebra length was recorded from the vertebra side that provided the greater measurement. FL was subsequently estimated using these measurements for all specimens as above.

Vertebra annuli were observed and measured by an experienced reader on the posterior centra of V35 and the anterior centra of V36. Annuli were interpreted as per Galtsoff (1952), Lee *et al.* (1983) and Rodríguez-Marín *et al.* (2006), such that one annulus was one groove (summer growth) and one ridge (winter growth). Because small growth increments and crowding at centrum edges result in difficulties differentiating BFT annuli at ages >8 (Rodríguez-Marín *et al.*, 2006), we adopted a conservative approach, measuring increment

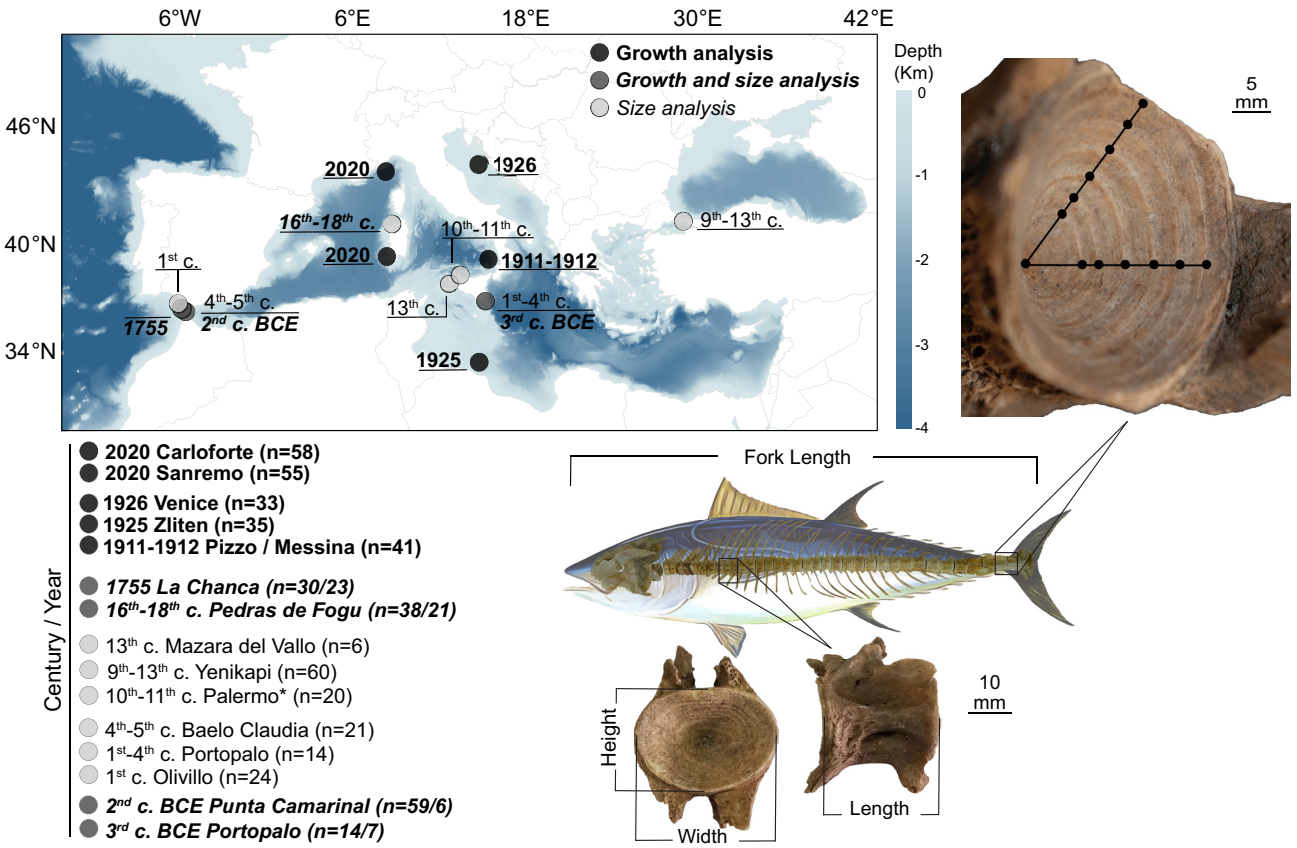

Figure 1. Map of modern, archival, and archaeological Atlantic bluefin tuna (*T. thynnus*) sample sites for length estimations (italic, light grey) and growth analyses (bold typeface, black) or both (italic boldface, dark grey). Map created using ESRI ArcMap (v.10.6, https://arcgis.com). Numbers (*n*) represent those used in growth analyses/length estimations. Points of annuli measurement (black dots) across distal and focal planes of vertebrae are illustrated using an example archaeological vertebra (35th) from 1755 ce Spain. The illustration indicates the FL measurements used and provides an example of a vertebra related to its vertebral position and measurements (height, width, and length) used to reconstruct FL. The scale bar (black bars) is an approximation only due to camera angle distortion. ∗ Palermo samples pertain to two different archaeological sites (see Supplementary Materials for details).

size between annuli 1–6 (Figure 1, Supplementary Figure S2). Staining was prohibited for the archaeological and archival samples, though experimentation with silver nitrate staining (Stevens, 1975) on modern specimens did not improve annuli readability. We found that illumination provided sufficient conditions for the interpretability of annuli by eye, which was occasionally further aided by rinsing centra with distilled water when annuli were less pronounced.

The study of archaeological and archived specimens also prohibited the cutting of vertebrae and thus increment size could not be measured using straight-edged digital callipers. The increment size was thus measured with specimens intact using a pair of dental callipers (curved, 20 mm max span) to the nearest 0.25 mm. The increment size was measured from the centrum apex (age 0), measuring to the outer winter ridge of the first annuli, then to the next outer winter ridge, and so on, thus recording annual growth from summer to summer. The increment size was measured and averaged across centrum focal and distal planes to account for variability in deformities, variability in the angle of measurement, and to ensure that annuli were complete throughout the centra following (Cullen *et al.*, 2021). Care was taken to avoid the measurement of false annuli, interpreted as being (1) less pronounced than annuli, (2) representing slower growth than expected, and (3) often not complete throughout the centrum. If annuli were not clearly observed, the specimen was not used in analyses (8 out of 121, 6%, modern, and 24 out of 133, 18% archived specimens collected). Sample groups were measured under the same conditions in random order to ensure measurement accuracy was not biased by space or time. To assess the reproducibility of our dataset, a second reader measured the increment size as above for a subset of specimens (93 out of 372, 25%), which reported high levels of correlation ($R^2 = 0.95$), and a measurement deviation of less than ±0.75 mm.

Growth estimation: statistical analyses

To statistically investigate significant differences in increment size at each age, we pooled samples into century groups (due to sample size limitations), applied one-way ANOVAs to V35 and V36 data separately, and interpreted the outputs using Tukey's Post-Hoc HSD test (except for the 3rd–2nd c. BCE samples due to small sample size). All statistical analyses were done using R v.4.1.3 (Team, 2013), thresholding significance at $p < 0.05$.

Variance in increment size was assessed using increasingly complex linear mixed-effects models (Morrongiello and Thresher, 2015) applied to V35 and V36 separately with the lmer function in the R package lme4 (Bates *et al.*, 2015). First, the optimal random model was determined: random effects

terms included intercept terms of the individual vertebra specimen (FishID), random effect term (Weisberg *et al.*, 2010), and sample (year, Table 1), and/or random slope terms of sample and age (of formation). Models were assessed using AICc (AIC corrected for small sample sizes, Burnham and Anderson, 2004) computed with the model.sel function in the AICcmodavg R package (Mazerolle, 2017). Mixed-effect models were then defined using the best-scoring random effect model, which included the intercept term FishID and slope of sample and age, for both the V35 and V36 dataset. Mixed-effect models were analysed for intrinsic effects and temporal effects, separately. First, intrinsic-effect models included vertebra length, width, or height (Figure 1). Second, temporal-effect models included sample or century. Century groupings combined 3rd c. BCE and 2nd c. BCE specimens together, and 1755 and 16th–18th c. specimens together. Full definition of random and mixed-effect terms can be found in the Supplementary (Supplementary Table S4). ANOVA and 95% confidence intervals were calculated for each model using the core functions *anova* and *confint* in R.

To qualitatively explore the influence of temperature on BFT growth, we collated a series of paleotemperature proxies and measurements to represent the spatiotemporal range of BFT statistically analysed. A western Mediterranean (Minorca Basin) sea surface temperature (SST) proxy was obtained from (Cisneros *et al.*, 2016), representing the stacked anomaly of 5 substrate core profiles. SST proxies were supplemented by the Hadley v4.1 SST northern Hemisphere anomaly for the years 1850–2021 CE (Kennedy *et al.*, 2019). Finally, a North Atlantic Oscillation (NAO) index proxy was obtained from (Faust *et al.*, 2016) and was supplemented by Hurrell's winter NAO index for the years 1865–2019 CE (Hurrell, 1995), which is presented as binned 3-year averages to maintain consistency with the temporal density of the NAO proxy. Temperature proxies and measurements were smoothed using the loess method in the ggplot2 function geom_smooth in R and illustrated with 95% CIs.

To assess the effect of resorption of bone on increment size and the ability to compare vertebrae of different sizes or ages, we first investigated the correlation between (log) vertebra centrum length, width, height, and (log) increment size. Second, we downsampled the 2020 sample, which had a lower mean FL than the other sample groups (Table 1, Supplementary Figure S5). We therefore removed the bottom 50% of individual FLs for the 2020 group and present these data for comparison (Supplementary Figure S6). Third, we included centra dimensions in intrinsic-effect models, detailed above.

Results

Historical catch-at-size estimation

FL was estimated for a total of 286 individuals (archaeological vertebrae), which illustrates that 3 rd c. BCE to 18 th c. BFT captured in eastern Atlantic and Mediterranean locations were between 90–284 cm FL (Figure 2, left) and were predominantly smaller than those captured in trap fisheries during the 20 th and 21 st centuries (Figure 2, right). In general, archaeological catch-at-size estimates range greatly at each site, and between all sites a tri-modal distribution is observed, with no clear temporal or spatial trend where the majority of BFT are distributed around peaks at ca. 120, 180 and 210 cm FL. Although the data are comparatively few, we note the catch of giant (250–300 cm FL) BFT in pre-Roman (Portopalo, Sicily) and Byzantine (Istanbul, Turkey) fisheries.

Pre-1950 ICCAT-collated BFT measurements (1915–1927) form a bi-modal distribution with peaks at ca. 110 and 220 cm FL (Figure 2, top right). BFT measured at these early 20 th c. traps represent a similar range to those captured throughout the 20 th and 21 st c. trap fisheries; however, during the periods 1956–1980 and 1980–2000, there is a greater relative catch of small (<100 cm FL) and very large (250 cm FL) BFT compared with the mean size frequency of these groups. After 1980, spatial variation was observed, in that Mediterranean trap catches contain a greater relative presence of small individuals (Figure 2, right). This is likely to be an artefact of the data where few traps are active and are in eastern Atlantic and Mediterranean locations known to be predominated by smaller adult individuals, for example, Sardinia (Addis *et al.*, 2016; Secci *et al.*, 2021).

Growth estimation

We produced a total of 1676 individual growth measurements across 372 samples spanning over two millennia and found that 21st c. BFT grew significantly ($p < 0.03$) faster at ages 1 and 2 than in the 20th c., and 16th–18th c., and that 20th c. BFT grew significantly faster at age 2 than the in the 16th–18th c. (Figure 3, Table S3a and b). This pattern is consistent across both V35 and V36 and coincides with stepwise SST and NAO increases with each period (Figure 3c). In general, the 16th–18th c. period comprises mostly of a negative NAO phase (Figure 3c, bottom), while estimates of SST (Figure 3c, top) are variable, but like those during the 1911–1926 period our archived samples pertain to. The early 20th c. sample dates, however, correspond to a positive NAO phase, which becomes more extreme at the 21st c., when SST measurements suggest conditions were a lot warmer than during both the 16th–18th, and early 20th century.

Across all samples, growth generally and logically decreased with age, where the biggest decreases were observed between the ages 1, 2, and 3, corresponding to annuli size measurements of ca. 4–5, 2.5–3.5, and 2–2.5 mm, respectively (Figure 3a and b). The increment sizes were consistent between V35 and V36. However, using V35, we detected a significantly ($p < 0.03$) slower growth at age 3 for the 16th–18th century group, and using V36, we detected a significantly faster growth for the 20th century group at age 4 (Figure 3a and b, Supplementary Table S3a, b). We observed a general pattern of similar but slower growth for the 3rd–2nd c. BCE group, compared with the remaining centuries. Large CIs and inconsistent patterns between V35 and V36 between the ages 3–6 hindered the interpretation of differences in growth between centuries, though growth between the ages 4–6 in 20th c. samples was increased compared with the remaining samples, and the general trajectory of the 21st c. samples was increased at ages 1, 2, and 3 but is decreased at ages 4, 5, and 6 (Figure 3a and b). Mean increment sizes, significance, and standard error bars for each sample group are presented in the Supplementary (Supplementary Figure S3, Table S3a and b).

Linear models with random effects (Supplementary Table S4, S5a) suggested that the variable century significantly explains increment size for the V35 (F = 5.6, 95% CI range:

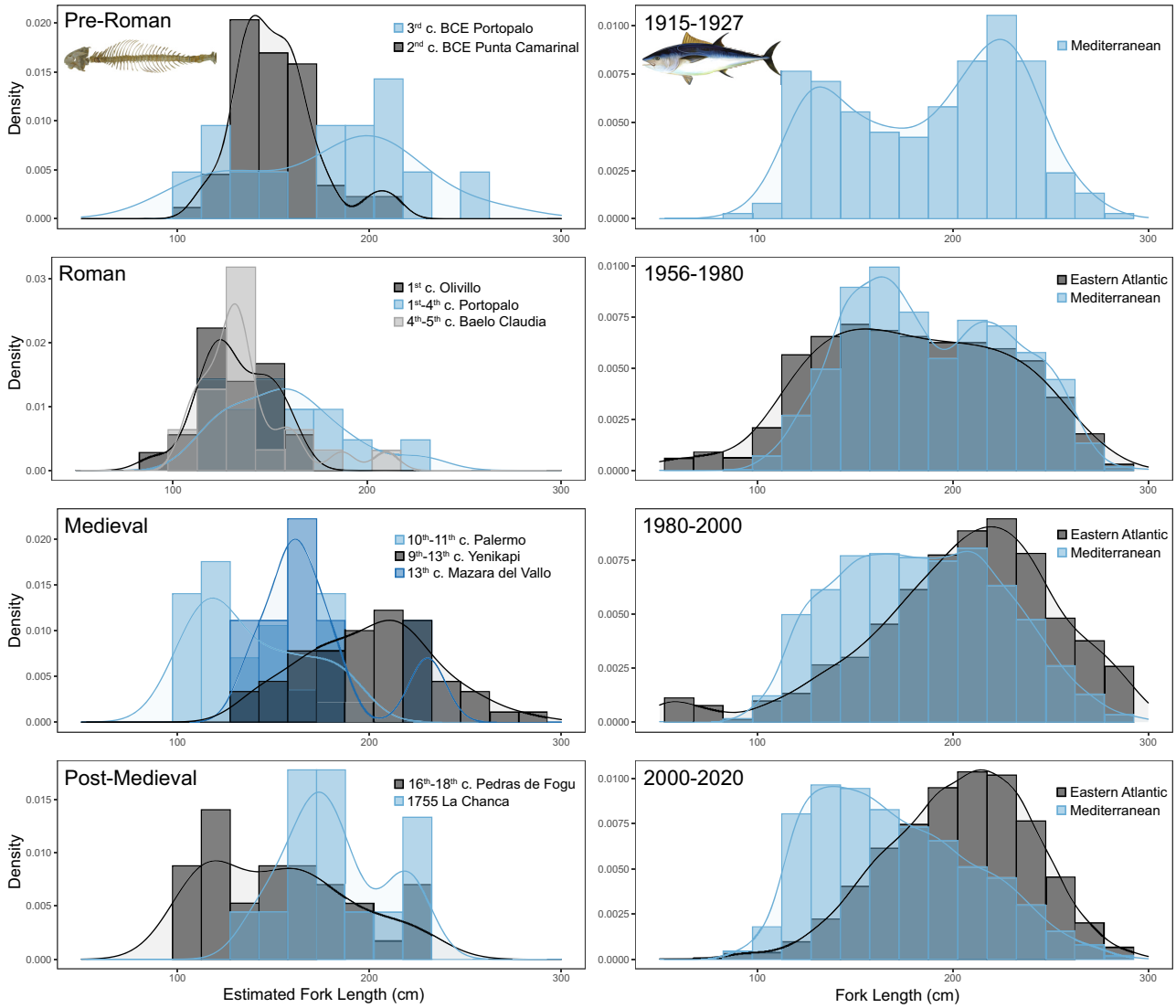

Figure 2. Size-at-capture density curves and histograms of estimated FL (cm) for archaeological Atlantic bluefin tuna (*T. thynnus*; BFT) vertebrae (left), shown per site and historical era (Pre-Roman, Roman, Medieval, Post-Medieval), and comparative density curves and histograms of BFT captured in trap fisheries, measured using straight FL from the ICCAT database and separated into multi-decadal groups (years ce). Each histogram size-class is 15 cm wide to approximately represent the (±10%) error in the length estimation methods for archaeological specimens. Mediterranean archaeological sites and historical and modern trap data are illustrated in colour, whereas eastern Atlantic and Bosporus archaeological sites and historical and modern trap data are illustrated in greyscale. For more details see Supplementary Table S2.

−0.27, 0.08) and V36 datasets (F = 9.6, 95% CI range −0.21, 0.23), as does sample (year), but to a slightly lower extent for both the V35 (F = 3.5, 95% CI range: −0.65, 0.51) and V36 dataset (F = 5.2, 95% CI range: −0.27, 0.23, Supplementary Table S5c). Linear models suggested no effect of vertebra length (F = 0.06–0.42, 95% CI range: −0.08, 0.16), width (F = 0.14–0.79, 95% CI range: −0.08, 0.16), or height (F = 0.05–0.17, 95% CI range: −0.12, 0.12) on Increment size (Supplementary Table S5b), which was also supported by the low variance explained by vertebra dimensions on increment size across all ages (R^2 = 0.01, Supplementary Figure S3). By altering the size composition of the dataset (removing small 21 st c. individuals), we noted no change in the interpretation of our results (Supplementary Figure S4).

Discussion

Temporal changes in BFT growth

Our results show that juvenile growth of BFT has sequentially and significantly increased between the 16th–18th, 20th, and 21st centuries. Our findings contradict those of Fromentin (2003), whose decrease in juvenile BFT weight-at-age appears not to be supported by the general trend of increasing juvenile fish growth over centuries found in the literature. We suspect this is because weight is a heavily variable trait, depending on sampling time, prey composition, and habitats foraged (Cort and Estruch, 2016). Likewise, we contradict evidence of no temporal change in BFT growth supposed by a century of length-at-age data (Cort *et al.*, 2014), probably because length-at-age studies used a variety of different elements and methods (Campana and Thorrold, 2001; Cullen *et al.*, 2021).

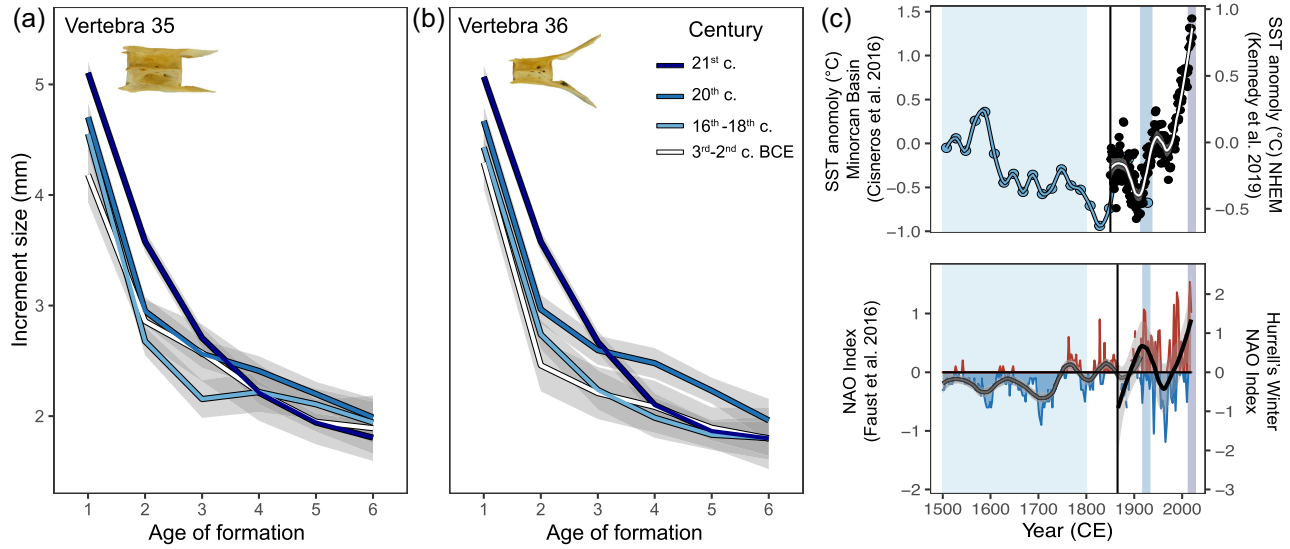

Figure 3. Temporal early-life growth estimates for Atlantic bluefin tuna (*T. thynnus*) using vertebra annuli measurements (a, b) and temperature proxies (c) for the Atlantic and Mediterranean presented as potential drivers of growth from the 16th c. to the present. (a, b) Smoothed increment sizes (mm) for each annuli (age of formation) measured in the 35th (a) and 36th (b) vertebrae (insets) are illustrated per "century" grouping, using the loess method geom_smooth function in R, grey shading indicates 95% confidence intervals. (c) The temperature proxies, collated between the years 1500–2019 ce (at the top panel) are; a SST proxy (blue dots and line, Cisneros *et al.*, 2016) and measurements (black dots, white line, Kennedy *et al.*, 2019) for the western Mediterranean and averages across the northern Hemisphere, respectively; and (at the bottom panel) a NAO proxy (grey line, Faust *et al.*, 2016) and Hurrell's Winter NAO Index (black line, Hurrell, 1995), positive values red, negative values blue: bottom panel, presented as smoothed using the same method as (a, b). Century sample time-points are indicated as whiskers between panels, and dashed lines (approximate sample dates: top, bottom panels) matching colours in b, using 1755 ce for the 16th–18th c. group, though the dating of the entire group is defined as between 16th and 18th century.

Figure 4. Depictions of Atlantic bluefin tuna (*T. thynnus*) from various artists, cropped to illustrate catch-at-size in (a) an ancient Greek era (6th c. bce) vase exhibited at the State Museum of Berlin (Germany), (b) 13th c. engraving depicting a tuna trap at Zahara de los Atunes (Spain) © Fundación Casa Medina Sidonia, (c) 16th c. engraving depicting a tuna trap at Cadiz (Spain) by the artist Georg Hoefnagel in 1572, (d) 18th c. engraving depicting a tuna trap at Trapani (Sicily, Italy) by the artist Jean-Pierre Louis Laurent Houël in (1782) and (e), an early 20th c. print in the newspaper "La Domenica del Corriere," published in Milan (Italy), 8th June 1900, depicting a tuna trap at Isola Piana (Sardinia, Italy). Depictions can be observed in full in Di Natale (2012).

Increased juvenile fish growth has been associated with increased temperature and decreased stock biomass in paleoecological studies on marine fishes (Geffen *et al.*, 2011; van der Sleen *et al.*, 2016; Denechaud *et al.*, 2020; Smoliński *et al.*, 2020; Vieira *et al.*, 2020; Pedersen *et al.*, 2022), supporting long-observed monthly and yearly trends that higher temperatures increase primary productivity (Moreno *et al.*, 2004) and the metabolic rate of fishes, while decreased competition at lower population densities increases fish growth (Brett, 1979; Beverton, 1995). A recent modelling study supports that BFT growth has increased during the past 60 years, driven by warming temperatures (Zhou, 2022). We find it equally plausible that recent increased growth at age 1 may reflect earlier spawning ontogenies because growth is enhanced during spring and summer months when BFT spawn (Mather *et al.*, 1995; Medina, 2020). This is a theory deserving of inves-

tigation due to its temperature-driven component (Fiksen and Reglero, 2022) and consequences on the reproductive output of BFT as a multiple-batch spawner (Medina, 2020).

In the closely-related southern bluefin tuna, increased juvenile growth was observed during 1960–90s, and was purportedly tightly linked with a reduction in biomass, rather than temperature (Jenkins *et al.*, 1991; Farley and Gunn, 2007). Indeed, early-life biomass will be even more reduced in size-truncated stocks since reproductive output scales strongly with body size (Medina, 2020). While we have no information on the biomass of eastern BFT during the 16th–18th c. and the early 20th c., it is reasonable to assume that BFT biomass has sequentially decreased in recent centuries due to the intensive trap catches and expansion of their fisheries into the Atlantic during the 19th c., and the extreme overexploitation that occurred especially during the late 20th c. (Porch *et al.*, 2019). While the eastern stock has recovered to 1970s levels in recent years, we suspect that it remains decreased from early 20th c. and pre-industrial levels both in abundance and mean body size (Andrews *et al.*, 2022b). Therefore, while increasing ocean temperatures and the prevalence of positive NAO phases coincide with the increases in juvenile we observed, we are unable to disentangle these effects from stock biomass, or indeed any other covariate for which data is unavailable, such as the eastern Mediterranean Transient, prey abundance, or predation (Di Natale *et al.*, 2017; Smoliński, 2019).

FIE is expected to, and has been shown to, increase juvenile growth and decrease mature growth due to an energetic tradeoff favouring earlier maturation and increased reproductive investment management (Law, 2000; Edeline *et al.*, 2007; Jørgensen *et al.*, 2007; Mollet *et al.*, 2007; Swain *et al.*, 2007; Neuheimer and Taggart, 2010; Saura *et al.*, 2010; Enberg *et al.*, 2012; Hollins *et al.*, 2018). FIE is therefore another potential explanator of increases in juvenile growth between the 16th–21st century. Given that we observed similar BFT growth between centuries at ages 4–6 (the first ages affected by reproductive investment), our data suggest that evolutionary forcing on BFT mature growth during the past five centuries related to size-selective harvesting is less likely. Although, as is often the case with limited paleoecological data and methods, these results must be interpreted with caution.

Increased growth, associated with plasticity responses to favourable environmental conditions, could, in theory, cancel out evolutionary size-selective harvesting effects; which decrease mature growth (Swain *et al.*, 2007; Heino *et al.*, 2008; Hutchings and Kuparinen, 2021). Furthermore, we cannot exclude the possibility that our methods, which necessarily limited our sample size and measurement precision, hindered the observation of a decrease in growth. Indeed, we observe a (non-significant) decrease in growth at ages 4–6 between the 20th and 21st c. but not between the 16th–18th c. and the 20th c., which appears to support our archaeological size estimations, such that large BFT were not preferentially extracted during the pre-industrial era. Given that the early 20th c. ICCAT size-frequency data resemble those of the latter 20th c., stock age or size composition had likely not been truncated by the early 20th century. Whereas by the 21st c., it appears to have been (Fromentin, 2009; MacKenzie *et al.*, 2009; Siskey *et al.*, 2016b).

Therefore, FIE may have indeed decreased growth for 21st c. ages 4–6 BFT, acting against enhanced growth at these ages as observed in the 20th c. BFT, which would be driven by other factors like temperature and biomass as for juvenile growth, or others such as skipped-spawning, which impact growth at reproductive ages (Jørgensen *et al.*, 2006; Aarestrup *et al.*, 2022). This pattern of increased juvenile growth and decreased mature growth is not unique to BFT among overexploited fish stocks (Smoliński *et al.*, 2020), and is deserving of careful consideration if we are to disentangle plastic and evolutionary effects on fish growth.

Smaller catch-at-size for the pre-industrial era

Our catch-at-size estimates preclude assessments of stock size structure because of estimation error (±10% FL), small sample size, and biases associated with archaeological recoveries (which sites and vertebra were available to study, and the number of fishing episodes they represent). Rather than being population-representative size-frequency data, instead these data inform us that prior to the 19th c., BFT catch-at-size was likely smaller than during the 20th and 21st c., which consequently implies that BFT exploitation was less intense prior to the 19th century. Historical depictions of BFT appear to support this thesis of a predominantly ca. 150 cm FL catch-at-size between ancient Greek and post-Medieval times (Figure 4 a–d), whereas BFT are depicted noticeably larger (ca. 200 cm FL), from the mid-19th c. onwards (Figure 4e). Indeed, this trend is consistent across scores of depictions summarized in Di Natale (2012).

We postulate that in locations other than narrow channels (e.g. the Bosporus), where large BFT (>200 cm FL) were well-known to frequent and migrate close to coasts (Cort *et al.*, 2013), large BFT were not routinely targeted and captured prior to the 19 th c., probably due to gear or worker limitations and market demand. From the Phoenician era onwards the predominant method of BFT capture in the Mediterranean was via tuna trap [for a review see García Vargas and Florido Corral (2007)], which were nets fixed or cast perpendicular to coasts, which intercepted migrations of BFT. During the 19 th and 20 th c., we postulate that tuna traps were extended further from the shore, facilitating the capture of deeper-migrating individuals. We suggest that at the sites studied herein, the largest BFT were not targeted due to the use of traps cast from the shore, or fixed in shallower waters where smaller BFT predominate (Mather *et al.*, 1995; Wilson and Block, 2009), but we cannot exclude the unlikely possibility other capture methods used for millennia such as handlines and driftnets, which would also target smaller, inshore individuals (Andrews *et al.*, 2022b).

We cannot rule out that the largest BFT bones were discarded on beaches, and are not represented in the archaeological record, or simply that large BFT did not migrate to the sites studied. Two of the sites studied (2nd c. BCE Punta Camarinal and 16th–18th c. Pedras de Fogu) were indeed processing centres directly on the back of beaches where BFT were captured, yet these sites did not yield large BFT. Sardinian sites (such as 16th–18th c. Pedras de Fogu) are however predominated by smaller BFT in modern traps (Addis *et al.*, 2016; Secci *et al.*, 2021), so clearly, archaeological approaches like ours limited by the number of individuals and sites require cautious interpretation. We suggest that further exploration of catch-at-size at additional post-medieval trap sites, especially during the 19th c., would better define the onset of a more-intense fixed trap fishery when large BFT were fished in greater frequency.

Study limitations

Due to the challenges of working with temporal samples, and the methods we were limited to, we could not produce growth rates to compare with other studies. Though our growth trajectories certainly resemble those of modern samples [e.g. Megalofonou and De Metrio (2000)], the methods we employed of measuring intact vertebrae up to age 6, result in reliable intra-study assessments of growth at each age only. Temporal studies of well-preserved otoliths will be required to estimate archaeological growth rates for BFT [e.g. Denechaud *et al.* (2020), Smoliński *et al.* (2020), Vieira *et al.* (2020)]. The use of otoliths will also aid in removing uncertainties about vertebra resorption. We found that increment size was not influenced by vertebra size, which on the one hand implies that annuli widths are not modified to a detectable level during resorption in BFT, but on the other hand that increment increases do not necessarily translate to increases in size for the whole vertebra and therefore FL. One explanation may be that increases in juvenile growth are met with decreased mature growth [see Smoliński (2019)]. It is possible we have largely escaped the effects of resorption due to working mostly with samples at early-life stages, since resorption has been shown to increase with age in BFT fin-spines (Santamaria *et al.*, 2015). Given that western and eastern BFT growth is not statistically different (Stewart *et al.*, 2022), it is unlikely that temporal trends were conflated by spatial differences within the eastern stock—though we cannot rule this out entirely. We attempted to limit spatial effects by collecting samples caught in relatively similar locations, and by pooling samples into century groupings. Albeit, no consistent spatial growth patterns have been observed in eastern BFT (Restrepo *et al.*, 2007; Cort *et al.*, 2014), likely as a result of wide-ranging migrations from age 1 (Dickhut *et al.*, 2009).

Conclusion

In summary, we provide novel evidence that BFT juvenile growth significantly increased between the 16 th–18 th, 20 th, and 21 st centuries and is correlated with warming SST's and NAO phases, and probably a decrease in stock biomass. An equally plausible explanation is that FIE contributed to increases in juvenile growth in favour of earlier maturation for the 20 th and 21 st century. Indeed, we found sparse evidence to suggest a long history of large (>200 cm FL) BFT capture. Rather, we postulate that size-selective fishing of BFT occurred from ca. 19 th century onwards when tuna traps were set further from the shore, and offshore fisheries developed. BFT growth remains a complex issue in need of further exploration to better define the onset of exploitation impacts and therefore, the recovery of the eastern BFT stock. Specifically, further study is required using fine-scale methods, that is, biochronological analyses of otoliths and adaptation genomics from 1900 onwards, to determine whether FIE is the driver of growth changes we observed between the early 20 th and 21 st century.

Acknowledgements

We would like to thank ICCAT and the GBYP Project, for collating and making available a database of BFT size records. Thanks to Jose Luis Cort for inspiration and assistance with size-at-age equations. Thanks to Ana Rita Viera for advice on linear modelling. Finally, we thank Emma Falkeid Eriksen for thoughtful discussions and the reviewers who improved the quality of this manuscript.

Supplementary Material

Supplementary material is available at the *ICESJMS* online version of the manuscript.

Data availability statement

Size estimation data is available in the Supplementary File Table S1. Raw growth data is available from the corresponding authors upon reasonable request.

Author contributions

A.J.A. designed the study. All authors collected samples for the study. A.J.A. performed the laboratory work. A.J.A. performed the statistical analyses. A.J.A., A.M.M., and F.T. wrote the paper. All authors reviewed the paper.

Funding

This work is a contribution to the https://tunaarchaeology.org project within the framework of the MSCA SeaChanges ITN, which was funded by EU Horizon 2020 [Grant Number: 813383]. This work also benefited from Spanish Ministry of Science funding [Grant Number: PID2020-118662GB-100].

Conflicts of interest

The authors declare no conflicts of interest exist.

References

Aarestrup, K., Baktoft, H., Birnie-Gauvin, K., Sundelöf, A., Cardinale, M., Quilez-Badia, G., Onandia, I. *et al.* 2022. First tagging data on large Atlantic bluefin tuna returning to Nordic waters suggest repeated behaviour and skipped spawning. Scientific reports, 12: 11772.

Addis, P., Secci, M., Pischedda, M., Laconcha, U., and Arrizabalaga, H. 2014. Geographic variation of body morphology of the Atlantic bluefin tuna, (*Thunnus thynnus*, Linnaeus, 1758). Journal of Applied Ichthyology, 30: 930–936.

Addis, P., Secci, M., Biancacci, C., Loddo, D., Cuccu, D., Palmas, F., and Sabatini, A. 2016. Reproductive status of Atlantic bluefin tuna, *thunnus thynnus*, during migration off the coast of Sardinia (western Mediterranean). Fisheries research, 181: 137–147.

Andrews, A. J., Mylona, D., Rivera-Charún, L., Winter, R., Onar, V., Siddiq, A. B., Tinti, F. *et al.* 2022a. Length estimation of Atlantic bluefin tuna (*Thunnus thynnus*) using vertebrae. International Journal of Osteoarchaeology, 32:645–653.

Andrews, A. J., Di Natale, A., Bernal-Casasola, D., Aniceti, V., Onar, V., Oueslati, T., Theodropoulou, T. *et al.* 2022b. Exploitation history of Atlantic bluefin tuna in the eastern Atlantic and Mediterranean—insights from ancient bones. ICES Journal of Marine Science, 79: 247–262.

Barrett, J. H. 2019. An environmental (pre)history of European fishing: past and future archaeological contributions to sustainable fisheries. Journal of Fish Biology, 94: 1033–1044.

Bates, D., Mächler, M., Bolker, B., and Walker, S. 2015. Fitting linear mixed-effects models using lme4. Journal Statistical. Software, 67: 1–48.

Beverton, R. J. H. 1995. Spatial limitation of population size; the concentration hypothesis. Netherlands Journal of Sea Research, 34: 1–6.

Bolle, L. J., Rijnsdorp, A. D., van Neer, W., Millner, R. S., van Leeuwen, P. I., Ervynck, A., Ayers, R. *et al.* 2004. Growth changes in plaice, cod, haddock and saithe in the North Sea: a comparison of (post-)medieval and present-day growth rates based on otolith measurements. Journal of Sea Research, 51: 313–328.

Brett, J. R. 1979. Environmental factors and growth. Fish Physiology, Vol. VIII. Bioenergetics and Growth.599–677,Academic Press. New York, USA.

Burnham, K. P., and Anderson, D. R. 2004. Multimodel inference: understanding AIC and BIC in model selection. Sociological Methods and Research, 33: 261–304.

Campana, S. E. 1990. How reliable are growth back-calculations based on otoliths? Canadian Journal of Fisheries and Aquatic Sciences, 47: 2219–2227.

Campana, S. E., and Thorrold, S. R. 2001. Otoliths, increments, and elements: keys to a comprehensive understanding of fish populations? Canadian Journal of Fisheries and Aquatic Sciences, 58: 30–38.

Cisneros, M., Cacho, I., Frigola, J., Canals, M., Masqué, P., Martrat, B., Casado, M. *et al.* 2016. Sea surface temperature variability in the central-western Mediterranean Sea during the last 2700 years: a multi-proxy and multi-record approach. Climate of the Past, 12: 849–869.

Corriero, A., Karakulak, S., Santamaria, N., Deflorio, M., Spedicato, D., Addis, P., Desantis, S. *et al.* 2005. Size and age at sexual maturity of female bluefin tuna (*Thunnus thynnus* L. 1758) from the Mediterranean Sea. Journal of Applied Ichthyology, 21: 483–486.

Cort, J. L. 1989. Biología y pesca del atún rojo, Thunnus thynnus (l.), del Mar Cantábrico. Doctoral Thesis. Universidad Complutense de Madrid. Madrid, Spain.

Cort, J. L. 2003. Age and growth of the bluefin tuna (*Thunnus thynnus*) of the Norheast Atlantic. Cahiers Options Méditerranéennes (CIHEAM),60: 45–49.

Cort, J. L., Deguara, S., Galaz, T., Mèlich, B., Artetxe, I., Arregi, I., Neilson, J. *et al.* 2013. Determination of L max for Atlantic bluefin Tuna, *Thunnus thynnus* (L.), from meta-analysis of published and available biometric data. Reviews in Fisheries Science, 21: 181–212.

Cort, J. L., Arregui, I., Estruch, V. D., and Deguara, S. 2014. Validation of the growth equation applicable to the Eastern Atlantic bluefin tuna, *Thunnus thynnus* (L.), using Lmax, tag-recapture, and first dorsal spine analysis. Reviews in Fisheries Science & Aquaculture, 22: 239–255.

Cort, J. L., and Estruch, V. D. 2016. Analysis of the length–weight relationships for the Western Atlantic Bluefin Tuna, *Thunnus thynnus* (L.). Reviews in Fisheries Science & Aquaculture, 24: 126–135.

Cullen, T. M., Brown, C. M., Chiba, K., Brink, K. S., Makovicky, P. J., and Evans, D. C. 2021. Growth variability, dimensional scaling, and the interpretation of osteohistological growth data. Biology Letters, 17: 20210383.

Czorlich, Y., Aykanat, T., Erkinaro, J., Orell, P., and Primmer, C.R., 2022. Rapid evolution in salmon life history induced by direct and indirect effects of fishing. Science, 376: 420–423.

Denechaud, C., Smoliński, S., Geffen, A. J., Godiksen, J. A., and Campana, S. E. 2020. A century of fish growth in relation to climate change, population dynamics and exploitation. Global Change Biology, 26: 5661–5678.

Dickhut, R. M., Deshpande, A. D., Cincinelli, A., Cochran, M. A., Corsolini, S., Brill, R. W., Secor, D. H. *et al.* 2009. Atlantic bluefin tuna (*Thunnus thynnus*) population dynamics delineated by organochlorine tracers. Environmental Science & Technology, 43: 8522–8527.

Di Natale. 2012. The iconography of tuna traps: essential information for the understanding of the technological evolution of this ancient fishery. Col. Vol. Sci. Pap. ICCAT, 67: 33–74.

Di Natale, A. 2014. The ancient distribution of bluefin tuna fishery: how coins can improve our knowledge. Col. Vol. Sci. Pap. ICCAT, 70: 2828–2844.

Di Natale, A., Tensek, S., and Paga, G. A. 2017. The disappearance of young-of-The-year bluefin tuna from The Mediterranean Coast in 2016: is it an effect of The climate change. Col. Vol. Sci. Pap. ICCAT, 74: 2850–2860.

Edeline, E., Carlson, S. M., Stige, L. C., Winfield, I. J., Fletcher, J. M., James, J. B., Haugen, T. O. *et al.* 2007. Trait changes in a harvested population are driven by a dynamic tug-of-war between natural and harvest selection. Proceedings of the National Academy of Sciences of the United States of America, 104: 15799–15804.

Enberg, K., Jørgensen, C., Dunlop, E. S., Varpe, Ø., Boukal, D. S., Baulier, L., Eliassen, S. *et al.* 2012. Fishing-induced evolution of growth: concepts, mechanisms and the empirical evidence. Marine Ecology, 33: 1–25.

Farley, J. H., and Gunn, J. S. 2007. Historical changes in juvenile southern bluefin tuna *Thunnus maccoyii* growth rates based on otolith measurements. Journal of Fish Biology, 71: 852–867.

Faust, J. C., Fabian, K., Milzer, G., Giraudeau, J., and Knies, J. 2016. Norwegian fjord sediments reveal NAO related winter temperature and precipitation changes of the past 2800 years. Earth and Planetary Science Letters, 435: 84–93.

Fiksen, Ø., and Reglero, P. 2022. Atlantic bluefin tuna spawn early to avoid metabolic meltdown in larvae. Ecology, 103: e03568.

Fromentin, J.-M. 2003. The East Atlantic and Mediterranean bluefin tuna stock management: uncertainties and alternatives. Scientia Marina, 67: 51–62.

Fromentin, J.-M. 2009. Lessons from the past: investigating historical data from bluefin tuna fisheries. Fish and Fisheries, 10: 197–216.

Galtsoff, P. S. 1952. Staining of growth rings in the vertebrae of Tuna (*Thunnus thynnus*). Copeia, 1952: 103–105

García Vargas, E., and Florido Corral, D. 2007. *The origin and development of tuna fishing nets (Almadrabas)*. In Proceedings of the International Workshop on Ancient Nets and Fishing Gear in Classical Antiquity. A First Approach. 205–227. Ed. by T. Bekker-Nielsen, and D. Bernal-Casasola Aarhus – Cádiz.

Geffen, A. J., Høie, H., Folkvord, A., Hufthammer, A. K., Andersson, C., Ninnemann, U., Pedersen, R. B. *et al.* 2011. High-latitude climate variability and its effect on fisheries resources as revealed by fossil cod otoliths. ICES Journal of Marine Science: Journal du Conseil, 68: 1081–1089.

Giorgi, F. 2006. Climate change hot-spots. Geophysical Research Letters, 33: 1–4.

Guillaud, E., Elleboode, R., Mahé, K., and Béarez, P. 2017. Estimation of age, growth and fishing season of a palaeolithic population of grayling (*Thymallus thymallus*) using scale analysis. International Journal of Osteoarchaeology, 27: 683–692.

Gunn, J. S., Clear, N. P., Carter, T. I., Rees, A. J., Stanley, C. A., Farley, J. H., and Kalish, J. M. 2008. Age and growth in southern bluefin tuna, *Thunnus maccoyii* (Castelnau): direct estimation from otoliths, scales and vertebrae. Fisheries Research, 92: 207–220.

Heino, M., Baulier, L., Boukal, D. S., Dunlop, E. S., Eliassen, S., Enberg, K., Jørgensen, C. *et al.* 2008. Evolution of growth in Gulf of St Lawrence cod? Proceedings of the Royal Society B: Biological Sciences, 275:1111–1112.

Hollins, J., Thambithurai, D., Koeck, B., Crespel, A., Bailey, D. M., Cooke, S. J., Lindström, J. *et al.* 2018. A physiological perspective on fisheries-induced evolution. Evolutionary applications, 11: 561–576.

Hurrell, J. W. 1995. Decadal trends in the north Atlantic oscillation: regional temperatures and precipitation. Science, 269: 676–679.

Hutchings, J. A., and Kuparinen, A. 2021. Throwing down a genomic gauntlet on fisheries-induced evolution. Proceedings of the National Academy of Sciences of the United States of America, 118:e2105319118.

ICCAT. 2007. Report of the 2006 Atlantic bluefin tuna stock assessment session. Col. Vol. Sci. Pap. ICCAT, 60: 652–880.

Jenkins, G. P., Young, J. W., and Davis, T. L. O. 1991. Density dependence of larval growth of a marine fish, the southern bluefin tuna, *Thunnus maccoyii*. Canadian Journal of Fisheries and Aquatic Sciences, 48: 1358–1363.

Jørgensen, C., Ernande, B., Fiksen, Ø., and Dieckmann, U. 2006. The logic of skipped spawning in fish. Canadian Journal of Fisheries and Aquatic Sciences, 63: 200–211.

Jørgensen, C., Enberg, K., Dunlop, E. S., Arlinghaus, R., Boukal, D. S., Brander, K., Ernande, B. *et al.* 2007. Ecology: managing evolving fish stocks. Science, 318: 1247–1248.

Kennedy, J. J., Rayner, N. A., Atkinson, C. P., and Killick, R. E. 2019. An ensemble data set of sea surface temperature change from 1850: the met office Hadley centre HadSST.4.0.0.0 data set. Journal of Geophysical Research, 124: 7719–7763.

Landa, J., Rodriguez-Marin, E., Luque, P. L., Ruiz, M., and Quelle, P. 2015. Growth of bluefin tuna (*Thunnus thynnus*) in the Northeastern Atlantic and Mediterranean based on back-calculation of dorsal fin spine annuli. Fisheries Research, 170: 190–198.

Law, R. 2000. Fishing, selection, and phenotypic evolution. ICES Journal of Marine Science: Journal du Conseil, 57: 659–668.

Lee, D.W., Prince, E.D., and Crow, M.E., 1983. Interpretation of growth bands on vertebrae and otoliths of Atlantic bluefin tuna, *Thunnus thynnus*. In Proceedings of the International Workshop on Age Determination of Oceanic Pelagic Fishes: Tunas, Billfishes, and Sharks, 8: 61–70. US Dep. Commer., NOAA Technical Report NMFS. Washington D.C., USA.

Lotze, H. K., Hoffmann, R., and Erlandson, J. 2014. Lessons from historical ecology and management. In The Sea, Volume 19: Ecosystem-Based Management. Harvard University Press. Massachusetts, USA.

MacKenzie, B. R., Mosegaard, H., and Rosenberg, A. A. 2009. Impending collapse of bluefin tuna in the northeast Atlantic and Mediterranean. Conservation letters, 2: 26–35.

Maschner, H. D. G., Betts, M. W., Reedy-Maschner, K. L., and Trites, A. W. 2008. A 4500-year time series of Pacific cod (*Gadus macrocephalus*) size and abundance: archaeology, oceanic regime shifts, and sustainable fisheries. Fishery Bulletin, 104: 386–394.

Mather, F. J., Mason, J. M., and Jones, A. C. 1995. . NOAA Technical Memorandum NMFS-SEFSC-370. National Oceanic and Atmospheric Administration. 165.https://repository.library.noaa.gov/view/noaa/8461. (last accessed October 1, 2022).

Mazerolle. 2017. AICcmodavg: model selection and multimodel inference based on (Q) AIC (c) (version 1.28). R Package. https://cran.r-project.org/web/packages/AICcmodavg/AICcmodavg.pdf. (last accessed October 1, 2022).

Medina, A. 2020. Reproduction of Atlantic bluefin tuna. Fish and Fisheries, 21: 1109–1119.

Megalofonou, P., and De Metrio, G. 2000. Age estimation and annulus-formation in dorsal spines of juvenile bluefin tuna, *Thunnus thynnus*, from the Mediterranean Sea. Journal of the Marine Biological Association of the United Kingdom, 80: 753–754.

Mollet, F. M., Kraak, S. B. M., and Rijnsdorp, A. D. 2007. Fisheries-induced evolutionary changes in maturation reaction norms in North Sea sole *Solea solea*. Marine Ecology Progress Series, 351: 189–199.

Moreno, A., Cacho, I., Canals, M., Grimalt, J. O., and Sanchez-Vidal, A. 2004. Millennial-scale variability in the productivity signal from the Alboran Sea record, Western Mediterranean Sea. Palaeogeography, Palaeoclimatology, Palaeoecology, 211: 205–219.

Morrongiello, J. R., and Thresher, R. E. 2015. A statistical framework to explore ontogenetic growth variation among individuals and populations: a marine fish example. Ecological Monographs, 85: 93–115.

Murua, H., Rodriguez-Marin, E., Neilson, J. D., Farley, J. H., and Juan-Jordá, M. J. 2017. Fast versus slow growing tuna species: age, growth, and implications for population dynamics and fisheries management. Reviews in Fish Biology and Fisheries, 27: 733–773.

Neilson, J. D. N., and Campana, S. E. C. 2008. A validated description of age and growth of western Atlantic bluefin tuna (*Thunnus thynnus*). Canadian Journal of Fisheries and Aquatic Sciences, 65, 1523–1527.

Neuheimer, A. B., and Taggart, C. T. 2010. Can changes in length-at-age and maturation timing in Scotian Shelf haddock (*Melanogrammus aeglefinus*) be explained by fishing? Canadian Journal of Fisheries and Aquatic Sciences, 67: 854–865.

Ólafsdóttir, G. Á., Pétursdóttir, G., Bárðarson, H., and Edvardsson, R. 2017. A millennium of north-east Atlantic cod juvenile growth trajectories inferred from archaeological otoliths. PLoS ONE, 12: e0187134.

Pagá Garcia, A., Palma, C., Di Natale, A., Tensek, S., Parrilla, A., and de Bruyn, P. 2017. Report on revised trap data recovered by ICCAT GBYP from phase 1 to phase 6. Col. Vol. Sci. Pap. ICCAT, 73: 2074–2098.

Pedersen, T., Amundsen, C., and Wickler, S. 2022. Characteristics of early Atlantic cod (*Gadus morhua* L.) catches based on otoliths recovered from archaeological excavations at medieval to early modern sites in northern Norway. ICES Journal of Marine Science: Journal du Conseil, 79, 2667–2681.

Pinsky, M. L., Eikeset, A. M., Helmerson, C., Bradbury, I. R., Bentzen, P., Morris, C., Gondek-Wyrozemska, A. T. *et al.* 2021. Genomic stability through time despite decades of exploitation in cod on both sides of the Atlantic. Proceedings of the National Academy of Sciences of the United States of America, 118:e2025453118.

Plank, M. J., Allen, M. S., Nims, R., and Ladefoged, T. N. 2018. Inferring fishing intensity from modern and archaeological size-frequency data. Journal of Archaeological Science, 93: 42–53.

Porch, C. E., Bonhommeau, S., Diaz, G. A., Haritz, A., and Melvin, G. 2019. The journey from overfishing to sustainability for Atlantic bluefin tuna, *Thunnus thynnus*. InThe future of bluefin tunas: ecology, fisheries management, and conservation, pp.3–44. Johns Hopkins University Press. Maryland, USA.

Restrepo, V. R., Rodríguez-Marín, E., Cort, J. L., and Rodríguez-Cabello, C. 2007. Are the growth curves currently used for Atlantic bluefin tuna statistically different? Col. Vol. Sci. Pap. ICCAT., 60: 1014–1026.

Rodrigues, A. S. L., Monsarrat, S., Charpentier, A., Brooks, T. M., Hoffmann, M., Reeves, R., Palomares, M. L. D. *et al.* 2019. Unshifting the baseline: a framework for documenting historical population changes and assessing long-term anthropogenic impacts. Philosophical transactions of the Royal Society of London. Series B, Biological sciences, 374: 20190220.

Rodríguez-Marín, E., Olafsdottir, D., Valeiras, J., Ruiz, M., Chosson-Pampoulie, V., and Rodríguez-Cabello, C. 2006. Ageing comparison from vertebrae and spines of bluefin tuna (*Thunnus thynnus*) coming from the same specimen. Col. Vol. Sci. Pap. ICCAT, 59: 868–876.

Rodríguez-Marín, E., Clear, N., Cort, J. L., Megalofonou, P., Neilson, J. D., dos Santos, M. N., Olafsdottir, D. *et al.* 2007. Report of the 2006 ICCAT workshop for bluefin tuna direct ageing. Col. Vol. Sci. Pap. ICCAT. 60: 1349–1392.

Rodríguez-Roda, J. 1964. Biología del atún, *Thunnus thynnus* (L.), de la costa sudatlántica de España. Consejo Superior de Investigaciones Científicas (España).

Rodríguez-Roda, J. 1967. Fecundidad del atún, *Thunnus thynnus* (L.), de la costa sudatlántica de España. Consejo Superior de Investigaciones Científicas (España).

Sanchez, G. M. 2020. Indigenous stewardship of marine and estuarine fisheries?: Reconstructing the ancient size of Pacific herring through linear regression models. Journal of Archaeological Science: Reports, 29: 102061.

Santamaria, N., Bello, G., Corriero, A., Deflorio, M., Vassallo-Agius, R., Bök, T., and De Metrio, G. 2009. Age and growth of Atlantic bluefin tuna, *Thunnus thynnus* (Osteichthyes: thunnidae), in the Mediterranean Sea. Journal of Applied Ichthyology, 25: 38–45.

Santamaria, N., Bello, G., Pousis, C., Vassallo-Agius, R., de la Gándara, F., and Corriero, A. 2015. Fin spine bone resorption in Atlantic bluefin tuna, *Thunnus thynnus*, and comparison between wild and captive-reared specimens. PLoS One, 10: e0121924.

Saura, M., Morán, P., Brotherstone, S., Caballero, A., Álvarez, J., and Villanueva, B. 2010. Predictions of response to selection caused by angling in a wild population of Atlantic salmon (*Salmo salar*). Freshwater Biology, 55: 923–930.

Secci, M., Palmas, F., Giglioli, A. A., Pasquini, V., Culurgioni, J., Sabatini, A., and Addis, P. 2021. Underwater tagging of the Atlantic bluefin tuna in the trap fishery of Sardinia (W Mediterranean). Fisheries Research, 233: 105747.

Sella, M. 1929. Migrazioni e habitat del tonno (*Thunnus thynnus*, L.) studiati col metodo degli ami, con osservazioni su l'accrescimento, sul regime delle tonnare ecc. Memoria, R. Comitato Talassografico Italiano,156: 511–542.

Siskey, M. R., Lyubchich, V., Liang, D., Piccoli, P. M., and Secor, D. H. 2016a. Periodicity of strontium: calcium across annuli further validates otolith-ageing for Atlantic bluefin tuna (*Thunnus thynnus*). Fisheries Research, 177: 13–17.

Siskey, M. R., Wilberg, M. J., Allman, R. J., Barnett, B. K., and Secor, D. H. 2016b. Forty years of fishing: changes in age structure and stock mixing in northwestern Atlantic bluefin tuna (*Thunnus thynnus*) associated with size-selective and long-term exploitation. ICES Journal of Marine Science: Journal du Conseil, 73: 2518–2528.

Smoliński, S. 2019. Sclerochronological approach for the identification of herring growth drivers in the Baltic Sea. Ecological Indicators, 101: 420–431.

Smoliński, S., Deplanque-Lasserre, J., Hjörleifsson, E., Geffen, A. J., Godiksen, J. A., and Campana, S. E. 2020. Century-long cod otolith biochronology reveals individual growth plasticity in response to temperature. Scientific Reports, 10: 16708.

Stevens, J. D. 1975. Vertebral rings as a means of age determination in the blue shark (*Prionace glauca* L.). Journal of the Marine Biological Association of the United Kingdom, 55: 657–665.

Stewart, N. D., Busawon, D. S., Rodriguez-Marin, E., Siskey, M., and Hanke, A. R. 2022. Applying mixed-effects growth models to back-calculated size-at-age data for Atlantic bluefin tuna (*Thunnus Thynnus*). Fisheries Research, 250: 106260.

Swain, D. P., Sinclair, A. F., and Mark Hanson, J. 2007. Evolutionary response to size-selective mortality in an exploited fish population. Proceedings. Biological sciences /The Royal Society, 274: 1015–1022.

Team, R. C. 2013. R development core team. RA Lang Environ Stat Comput, 55: 275–286.

Therkildsen, N. O., Wilder, A. P., Conover, D. O., Munch, S. B., Baumann, H., and Palumbi, S. R. 2019. Contrasting genomic shifts underlie parallel phenotypic evolution in response to fishing. Science, 365: 487–490.

van der Sleen, P., Dzaugis, M. P., Gentry, C., Hall, W. P., Hamilton, V., Helser, T. E., Matta, M. E. *et al.* 2016. Long-term Bering Sea environmental variability revealed by a centennial-length biochronology of Pacific ocean perch *Sebastes alutus*. Climate Research, 71: 33–45.

Van Neer, W., Löugas, L., and Rijnsdorp, A. D. 1999. Reconstructing age distribution, season of capture and growth rate of fish from archaeological sites based on otoliths and vertebrae. International Journal of Osteoarchaeology, 9 : 116–130.

Vieira, A. R., Dores, S., Azevedo, M., and Tanner, S. E. 2020. Otolith increment width-based chronologies disclose temperature and density-dependent effects on demersal fish growth. ICES Journal of Marine Science: Journal du Conseil, 77: 633–644.

Weisberg, S., Spangler, G., and Richmond, L. S. 2010. Mixed effects models for fish growth. Canadian Journal of Fisheries and Aquatic Sciences, 67: 269–277.

Wilson, S. G., and Block, B. A. 2009. Habitat use in Atlantic bluefin tuna *Thunnus thynnus* inferred from diving behavior. Endangered Species Research, 10: 355–367.

Zhou, C., 2022. Somatic growth of Atlantic bluefin tuna (*Thunnus thynnus*) under global climate variability: evidence from over 60 years of daily resolved growth increments with a simulation study. Canadian Journal of Fisheries and Aquatic Sciences, 79: 642–651.

Handling Editor: Allen Hia Andrews